J BONE ONCOL 35 (2022) 100439

Contents lists available at ScienceDirect

Journal of Bone Oncology

journal homepage: www.elsevier.com/locate/jbo

Research Paper

Pexmetinib suppresses osteoclast formation and breast cancer induced osteolysis via P38/STAT3 signal pathway

Zhiwei Jie [a,b,1], Shiyu Wang [a,b,1], Qingliang Ma [a,b], Yang Shen [a,b], Xiangde Zhao [a,b], Hejun Yu [a,b], Ziang Xie [a,b,*], Chao Jiang [a,b,*]

[a] Department of Orthopaedics, Sir Run Run Shaw Hospital, Zhejiang University School of Medicine, Hangzhou, China
[b] Key Laboratory of Musculoskeletal System Degeneration and Regeneration Translational Research of Zhejiang Province, Hangzhou, China

ARTICLE INFO

Keywords:
P38 mitogen-activated protein kinase
Pexmetinib
Osteoclast
Breast cancer
Osteolysis

ABSTRACT

Breast cancer metastases to the bone can lead to a series of bone-related events that seriously affect the quality of life. Pexmetinib, a novel p38 mitogen-activated protein kinase (p38) inhibitor that has been evaluated in phase I clinical trials for myelodysplastic syndrome, but the effects of Pexmetinib on breast cancer induced osteolysis haven't been explored. Here, we found that Pexmetinib inhibited receptor activator of nuclear factor-κB ligand-induced osteoclast formation and bone resorption *in vitro*. Pexmetinib suppressed p38-mediated signal transducer and activator of transcription 3 (STAT3), which direct regulated transcription of the nuclear factor of activated T cells 1 (NFATc1), leading to reduced osteoclast formation. Moreover, Pexmetinib exerted anti-tumor effects in breast cancer cells *in vitro* via suppressing p38-mediated STAT3 activation and matrix metalloproteinases (MMPs) expression. Furthermore, Pexmetinib suppressed breast cancer-associated osteolysis *in vivo*. These results suggest that Pexmetinib may be a promising drug for the treatment of breast cancer-induced osteolysis.

1. Introduction

Breast cancer is the most common cancer in women, and the skeleton is the most common target tissue for breast cancer metastases[1]. Breast cancer bone metastases can cause osteolytic lesions that, in turn, cause pathological fractures, hypercalcemia, intolerable bone pain, and a series of bone-related events that seriously affect the quality of life[2]. Some studies have been identified that breast cancer bone metastases induced excessive activation of osteoclasts is considered to be the main cause of osteolysis[3].Breast cancer cells can directly secrete the receptor activator of nuclear factor-κB ligand (RANKL), or cytokines (including the parathyroid hormone-related protein, tumor necrosis factor (TNF) alpha, macrophage colony-stimulating factor(M−CSF), and interleukin-1) stimulate RANKL secretion of osteoblasts in the bone matrix[4]. RANKL belongs to the tumor necrosis factor superfamily, and is critical for osteoclast activation *in vivo*. RANKL recruits TNF receptor-associated factor 6 via binding to its receptor RANK on the surface of osteoclast precursor cells, activating effectors such as nuclear factor-κB and mitogen-activated protein kinases (MAPKs), including extracellular signal-regulated kinase (ERK)1/2, p38 MAPK, and c-jun N-terminal kinase (JNK), ultimately leading to activation of activator protein-1 and the nuclear factor of activated T cells 1 (NFATc1)[5]. NFATc1 is a key transcription factor that regulates genes related to osteoclast differentiation, such as tartrate-resistant alkaline phosphatase (*TRAP*), dendritic cell-specific transmembrane protein (*DC-Stamp*), and cathepsin K (*CTSK*), ultimately determines the progress of osteoclast differentiation and function[6]. In addition, combined with bone destruction, various cytokines such as transforming growth factor-β (TGF-β) and insulin-like growth factor-1 (IGF-1), are released to promote the proliferation and invasion of tumor cells, thereby forming a vicious cycle of mutual promotion between osteoclasts and tumor cells[7]. Breaking the vicious cycle may be a promising direction for treatment of breast cancer-induced osteolysis. Currently, the osteoclast apoptosis stimulator, bisphosphonates is known as treating breast cancer-induced bone diseases[8]. Unfortunately, many studies have shown that the long-term use of bisphosphonates can inhibit the natural regeneration of bone tissue, causing non-spinal fractures in patients such as delayed union and femoral shaft fractures[9]. Thus, there is urgent need to develop more safe and effective therapeutic agents for treating breast cancer-induced osteolysis.

* Corresponding authors.
E-mail addresses: ziang_xie@zju.edu.cn (Z. Xie), 3319001@zju.edu.cn (C. Jiang).
[1] These authors contributed equally to this work.

https://doi.org/10.1016/j.jbo.2022.100439
Received 12 December 2021; Received in revised form 15 May 2022; Accepted 9 June 2022
Available online 11 June 2022

The MAPKs are a class of serine/threonine kinases involved in many cellular activities such as cell proliferation, differentiation, invasion, migration, and death[10]. Many studies have been reported that p38 MAPK is involved in osteoclast differentiation under RANKL treatment [11]. Moreover, the p38 MAPK-mediated signaling pathway has also been shown to play an indispensable role in breast cancer bone metastasis[12]. Pexmetinib is a novel inhibitor of p38 MAPK and has been investigated in phase I clinical trials for treating myelodysplastic syndrome[13], indicating that Pexmetinib has a good clinical application prospect. In this study, we demonstrated the efficacy of Pexmetinib on osteoclastogenesis and breast cancer cells *in vitro*, and found Pexmetinib can be used as an alternative drug for the treatment of osteolysis through animal model *in vivo*.

2. Materials and methods

2.1. Ethics approval

The animal experiments in this study were performed in accordance with the principles and procedures of the National Institutes of Health (NIH) Guide for the Care and Use of Laboratory Animals and the guidelines for animal treatment of Sir Run Run Shaw Hospital. All experimental protocols in this study were approved by the Ethics Committee of Sir Run Run Shaw Hospital.

2.2. Materials and main reagents

Pexmetinib was from Selleck Chemicals (Houston, Texas, USA). DMSO were purchased from Sigma-Aldrich (St. Louis, MO, USA). α-MEM (Eagle's minimal essential medium with Alpha Modification), dulbecco's modified eagle medium (DMEM), fetal bovine serum (FBS), and penicillin/streptomycin were purchased from Gibco-BRL. CCK-8 (Cell Counting Kit-8) was obtained from Dojindo Molecular Technology (Kumamoto, Japan). Recombinant soluble mouse M−CSF, mouse RANKL and Colivelin were obtained from R&D Systems (Minneapolis, MN, USA). All experiments were performed in the absence of visible light to prevent photosensitivity. Pexmetinib was diluted in cell culture medium so that DMSO comprised $< 0.1\%$ of the total volume. Meanwhile, 0.1% DMSO as a control group *in vitro*. Specific antibodies against ERK (extracellular signal-regulated kinase, 1:1000), JNK (c-Jun N-terminal kinase, 1:1000), p38 (1:1000), phosphorylated p-ERK (Thr202/Tyr204, 1:1000), p-JNK (Thr183/Tyr185, 1:1000), p-p38 (Thr180/Tyr182, 1:1000), STAT3 (1:1000), p-STAT3 (Tyr705, 1:1000), NFATc1 (1:1000) and GAPDH (1:10000) were obtained from Cell Signaling Technology (Boston, USA), and antibodies against TRAP (1:1000), MMP-2 (1:1000) and MMP-9 (1:1000) were purchased from Abcam (Cambridge, UK). TRAP staining kit and all other reagents were purchased from Sigma-Aldrich, unless otherwise stated.

2.3. Cell culture

Primary bone marrow macrophage cells (BMMs) were isolated from the six-week male C57BL/6 mice. After sacrificed, the femur and tibia of mice were taken out. The muscle tissues on the bone surface were removed, then both ends of the femur and tibia were cut off. The bone marrow was washed to the cell culture dish by the α-MEM medium containing 10% FBS, 100U/mL penicillin/streptomycin and 25 ng/ml M−CSF. We changed the medium every 48 h until the cells reached 80–90 % of density. After washed with PBS buffer, cells were digested by 0.25% trypsin for several minutes. The α-MEM medium was added, and the cell suspension was centrifugated at 800 rpm for 5 min at room temperature. After the cell pellets were pipetted and mixed evenly, BMMs were seeded in the cell culture dish for subsequent experiments. RAW264.7 cells were obtained from American Type Culture Collection, and human breast cancer cell line MDA-MB-231 was a gift from Dr. Linbo Wang (Sir Run Run Shaw Hospital, Zhejiang University), as described previously [15]. In brief, cells were cultured in DMEM with 10% FBS in a humidified atmosphere of 5% CO2 at 37 °C. The complete medium was changed every other day. All cell lines were tested and were free of mycoplasma.

2.4. In vitro osteoclastogenesis

BMMs were seeded in 96-well plates at the density of 8×10^3 cells per well. After 24-hours culture in the cell incubator, BMMs were then cultured by osteoclast differentiation medium (unless otherwise specified, osteoclast differentiation medium below refers to α-MEM containing RANKL (50 ng/mL) and M−CSF (25 ng/mL)). Meanwhile, cells were treated by different doses of Pexmetinib (0, 0.1, 0.2, 0.4 μM) at the same time. The 0 μM of Pexmetinib group added with 0.1% DMSO was set as the control group. When mature osteoclasts were observed in the control group, we fixed cells with 4% paraformaldehyde, then stained cells by TRAP. Cells with more than 3 nuclei that are positive for TRAP staining are considered as osteoclasts.

2.5. Quantitative real-time PCR

After seeded into 12-well plate, BMMs were treated without or with Pexmetinib (0.1, 0.2, 0.4 μM) for 5 days in the osteoclast differentiation medium. After that, add 1 ml TRIzon Reagent to each well and lyse by blowing repeatedly. Then we performed the total RNA extraction by an ultrapure RNA kit (CWbio, Beijing, China).

The extracted total cellular RNA was used for subsequent reverse transcription according to High-Capacity cDNA Reverse Transcription Kit from Applied Biosystems. RT-PCR were performed under SYBR Premix Ex Tag kit (TakaRa Biotechnology) in an ABI Prism 7500 system (Applied Biosystems, Foster City, CA) to further quantify the expression of genes. The primer sequences used in this study were as follows: 5′-ACCCAGAAGACTGT GGATG-3′ (forward), 5′-CACATTGGGGGTAG-GAACAC-3′ (reverse) for mouse GAPDH; 5-′CCAGTCAAGAGCATCAGCAA-3′ (forward), 5′-AAGTAGTGCAGCCCG-GAGTA-3′ (reverse) for mouse c-Fos; 5′-CCGTTGCTTCCAGAAAATAA CA-3′ (forward), 5′-CCGTTGCTTCCAGAAAATAACA-3′ (reverse) for mouse NFATc1; 5′-CTGGA GTGCACGATGCCAGCGACA-3′ (forward), 5′-TCCGTGCTCGGCGATGGACCAGA-3′ (reverse) for mouse TRAP; 5′-AAAACCCTTGGGCTGTTCTT-3′ (forward), 5′-AAT CATGGAC-GACTCCTTGG-3′ (reverse) for mouse DC-STAMP; 5′-CTTCCAATACGT GCAGCAGA-3′ (forward), 5′-TCTTCAGGGCTTTCTCGTTC-3′ (reverse) for mouse CTSK; 5′-AAAGGCAGCGTTAGCCAGAA-3′ (forward), 5′-GTCCGTGAGGTTG GAGGTTT-3′ (reverse) for mouse MMP-9; 5′-TGTGGG CATCAATGGATTTGG-3′, 5′-ACACCATGTATTCCGGGTCAAT-3′ (reverse) for human GAPDH; 5′-GACGCAG ACATCGTCATCCA-3′ (forward), 5′-CACAACTCGTCA TCGTCGAAA-3′ (reverse) for human MMP-9; 5′-TTGATGGCATCGCTCAGATC-3′ (forward), 5′-TTGTCACGTGG CGTCACAGT-3′ (reverse) for human MMP-2. The value was normalized to the GAPDH. Fold change expression of genes was calculated using the $2^{-\Delta\Delta Ct}$ method. The quantity of each target was normalized to GAPDH.

2.6. Western blot analysis

BMMs were seeded into 6-well plates for different treatment. Cells were washed by PBS, then RIPA lysis buffer (FdBio, Hangzhou, China) mixed with protease inhibitors (FdBio, 1:100) was added to lyse cells at 4 ℃ for 60 min. The cell lysate was collected and centrifuged at 12000 rpm at 4 °C for 15 min. The supernatant was collected as protein sample. The BCA method (Beyotime, Shanghai, China) was done to determine the concentration of protein. After that, we added 4 × SDS-PAGE loading buffer to each sample and denatured the protein at 100 °C for 5 ~ 10 min. The protein samples were used for SDS-PAGE gel electrophoresis, and transferred to the PVDF membrane. The PVDF membrane was blocked in TBST (50 mM Tris, pH 7.6; 150 mM NaCl; 0.1%

Tween 20) containing 5% skimmed milk for 1 h at room temperature. Subsequently, the blocked PVDF membrane was incubated with diluted related primary antibody at 4 °C for 12 h. Then the membrane was washed 3 times with TBST, each time for 10–15 min. Next, the membrane was further incubated with secondary antibody corresponding to the species of primary antibody for 60 min at room temperature. After washed three times by TBST, membranes were finally obtained using ECL developer solution under Bio-Ras Imaging System. The gray levels of captured images were analyzed by ImageJ.

2.7. In vitro bone absorption assay of osteoclast

After sterilization, the bovine bone slices were placed in 96-well plate. BMMs were seeded on the bovine bone slices, or the observation well without bone slices at a density of 8×10^3 per well. The cells were cultured with osteoclast differentiation medium until mature osteoclasts formed in the observation well. Then we treated osteoclasts on the bovine bone slices with different doses of Pexmetinib (0, 0.1, 0.2, 0.4 μM) for another 3 days. After washing with PBS, the bovine bone slices were taken out and observed using a scanning electron microscope (FEI Quanta 250). The quantitative analysis of the resorption area of bovine bone slices was performed by ImageJ software ([National Institutes of Health (NIH), Bethesda, Maryland, USA]).

2.8. Chromatin immunoprecipitation (ChIP) assays

The ChIP experiments were mainly carried out according to the Simple Chip Chromatin IP Kit. In brief, RAW264.7 cells were stimulated with or without RANKL (50 ng/mL) for 48 h, and then treated by 1% formaldehyde at 37 °C for 10 min to crosslink DNA and protein. After washed by PBS, the lysis buffer containing protease inhibitors was used to lyse cells. The lysed cell sample was sonicated to separate DNA and cell debris. After that, chromatin was digested by nuclease to obtain chromatin fragments. The chromatin fragments were incubated with specific STAT3 antibody or IgG antibody overnight for immunoprecipitation, then further incubated with ChIP-specific A/G agarose beads at 4 °C for 2 h. After multiple washings, the DNA-protein complex was extracted and purified, then finally tested by PCR.

2.9. Apoptosis assay

Cells were identified using an Annexin V-fluorescein Isothiocyanate (FITC)/PI Cell Apoptosis Kit (Invitrogen), according to the manufacturer's protocol. The cells were washed with PBS for twice times. Then, cells were incubated with 100 μl of 1 × annexin binding buffer containing 5 μl of annexin V-FITC and 1 μl of PI in the dark for 15 min before being analyzed with flow cytometry within the subsequent 30 min.

2.10. Transwell assay

The Transwell assay was used for examination of invasion and migration ability of MDA-MB-231 cells. We applied a layer of Matrigel Basement Membrane Matrigel (100 ug/m2) to the upper basement membrane at the bottom of the transwell chamber at 37 °C for 6 h (migration assay omit this step). The cells were pretreated for 12 h in serum-free culture. After digested, MDA-MB-231 cells about 5×10^4 were seeded in the upper chamber of the transwell and cultured in serum-free culture. At the same time, cell medium containing 10% FBS was added to the lower chamber of the chamber. The transwell chamber were incubated in a cell incubator as descripted before. Then the cells adhered on the bottom surface were fixed with 4% paraformaldehyde and stained with crystal violet at room temperature for 15 min. After washing with PBS several times, the light microscope was performed to observe cells. The number of cells was quantified by using ImageJ software.

2.11. Breast cancer bone metastasis induced osteolysis model

We randomly divided 15 mice into 3 groups: Sham group, Vehicle group, and Pb group. MDA-MB-231 cells were digested and washed by DMEM medium. Then the MDA-MB-231 cells suspension was (1×10^6/mL, volume 100ul) injected into the tibia plateau of BALB/c nu/nu mice in the Vehicle group and the Pb group. Mice in Sham group was injected by PBS. After that, the Vehicle group and Pb group were respectively intraperitoneally injected with PBS and Pexmetinib (10 mg/kg) every three days for one month. Finally, all mice were sacrificed, and tibia specimens were fixed in 4% paraformaldehyde for further micro-CT scan and histological analysis.

2.12. Micro-CT scanning

As descripted in a previous study[14], A high-resolution micro-CT scanner (Skyscan 1072; Skyscan, Aartselaar, Belgium) was performed to scan and analyze the fixed tibia of mice. The scanning layer was 9um, and the X-ray energy was set to 80 kV and 800uA. After scanning, three-dimensional reconstruction of each sample was done. In addition, The resident reconstruction program (SkyScan) analyze the structural parameters, including bone volume per tissue volume (BV/TV), number (Tb.N), and separation (Tb.Sp).

2.13. Bone histomorphometry and immunohistochemical analysis

The fixed tibia specimens of mice were immersed in 10% EDTA for 3 weeks to decalcify. After decalcification, they were embedded in paraffin and sectioned. The tibia sections were stained by H&E, TRAP and p-STAT3 immunohistochemical assays.

2.14. Statistical analysis

All data are expressed as mean ± standard error of the mean (SEM). Statistical analyses were performed using Prism 6 (GraphPad Software, Inc., San Diego, CA, USA). Statistical differences were assessed by Student's *t*-test or one-way ANOVA followed by Tukey's post hoc analysis where appropriate. $P < 0.05$ was considered significant.

3. Results

3.1. Pexmetinib inhibited RANKL-induced osteoclast formation in vitro

To find potential strategies for treating breast cancer-induced osteolysis, we first evaluated the effect of Pexmetinib on osteoclast differentiation. As shown in Fig. 1**A-B**, Pexmetinib exhibited no effects on BMMs proliferation at a dose no more than 1.6 μM. And the inhibitory concentration (IC)50 value of Pexmetinib at 96 h was shown to be 4.144 μM (Fig. 1**C**). In Fig. 1**D**, TRAP-positive multinucleated osteoclasts were observed after treatment with RANKL for 5 days. However, osteoclast number and area were both suppressed following Pexmetinib (0.1–0.4 μM) treatment in a concentration-dependent manner (Fig. 1**D-E**). Next, we investigated whether Pexmetinib impaired the osteoclastic bone resorption process. The mature osteoclasts on the bone slices was treat with or without Pexmetinib for 3 days. As shown in Fig. 1**G**, bone resorption area observed in the control group was much more than resorption area observed in the Pexmetinib treated groups. By the quantity analysis, the resorption area was reduced about 45% in the 0.1 μM Pexmetinib treatment group compared to the control group, and reduced about 88% in the 0.4 μM treatment group (Fig. 1**H**). Together, we found the inhibitory effect of Pexmetinib on osteoclastogenesis and osteoclastic bone resorption.

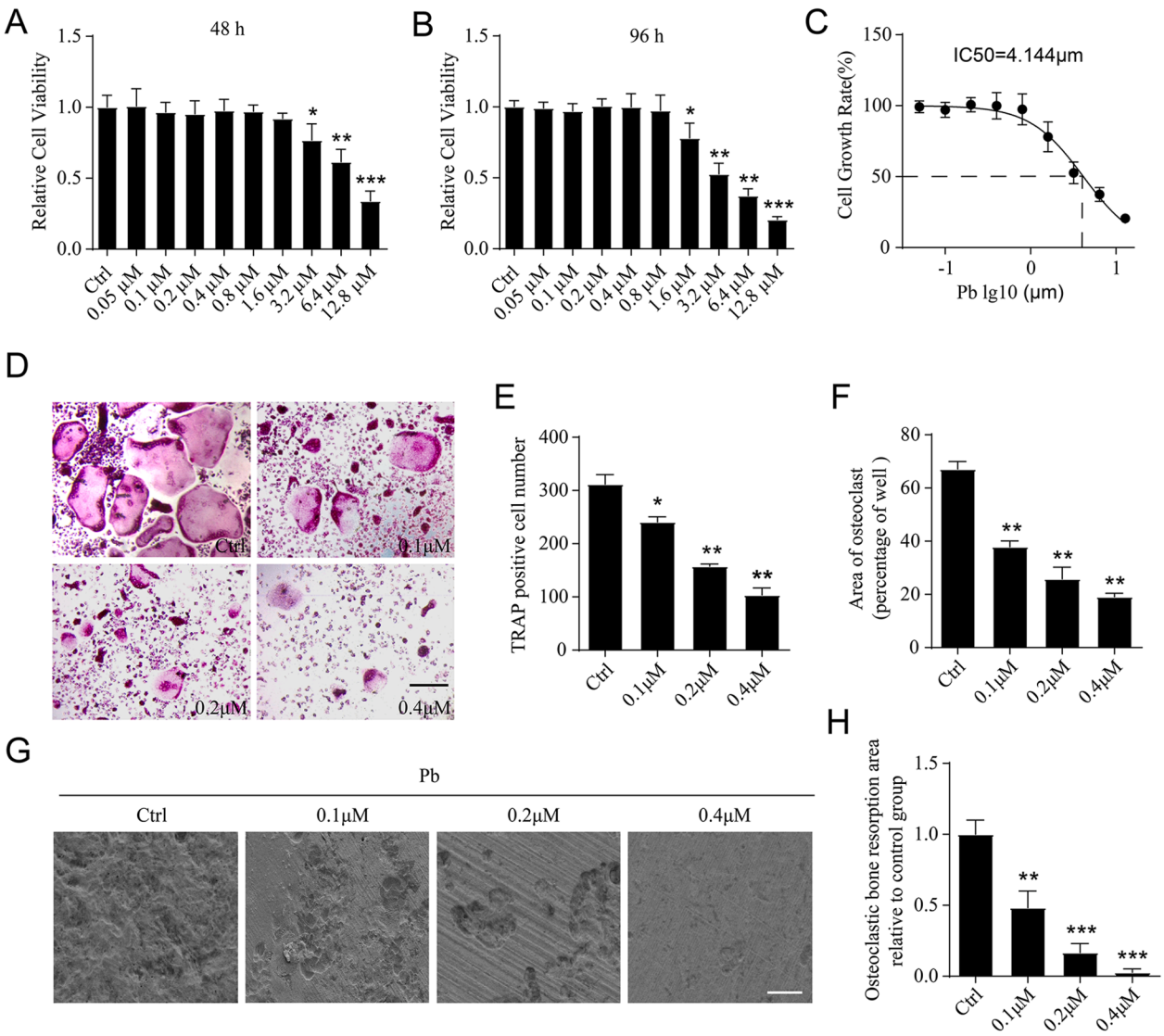

Fig. 1. Pexmetinib inhibits RANKL-induced osteoclastogenesis *in vitro*. (A, B) Cell viability of Pexmetinib treated BMMs tested by CCK-8 assays at 48 and 96 h. **(C)** The IC50 value of Pexmetinib at 96 h on BMMs **(D)** BMMs were cultured in osteoclast differentiation medium for 5 days followed by different concentrations of Pexmetinib (0, 0.1, 0.2, 0.4 μM). **(E-F)** The number and areas of osteoclasts were measured by imageJ. **(G)** Bone-resorption pits were visualized by scanning electron microscopy following treatment with different concentrations of Pexmetinib. **(H)** Resorption pit areas were measured using Image J and normalized relative to the control group. Scale bar = 100 μm, *P < 0.05; **P < 0.01. Data are expressed as means ± SEM, n = 5.

3.2. Pexmetinib suppressed the expression of osteoclastic genes and proteins.

To further assess the inhibitory effects of Pexmetinib on osteoclastogenesis, we examined the expression of RANKL-induced osteoclast-specific genes, including *Nfatc1*, *Trap*, *Dc-stamp*, *Ctsk*, *Atp6v0d2* and *Mmp9* under Pexmetinib treatment. As shown in Fig. 2**A-F**, the upregulated expression of osteoclast differentiation related genes under RANKL stimulation was significantly inhibited by Pexmetinib treatment (0.1, 0.2, 0.4 μM). Furthermore, we focused on the protein expression of NFATc1, a very important transcription factor in osteoclast differentiation. Western blotting results demonstrated that the protein expression of NFATc1 and CTSK increased significantly in the 3 days and 5 days during osteoclast differentiation in control group (Fig. 2**G-I**). However, compared with the control group, the expression of NFATc1 and CTSK decreased significantly in the Pexmetinib treatment group (Fig. 2**G-I**). These results indicated that NFATc1 may be a potential target of Pexmetinib on osteoclast differentiation.

3.3. Pexmetinib impaired p38-STAT3-NFAc1 axis during osteoclastogenesis

To further claim the mechanisms of which Pexmetinib affects NFATc1 expression. As shown in Fig. 3**A-B**, Pexmetinib specifically attenuated P38 phosphorylation but not JNK and ERK1/2 phosphorylation under RANKL stimulation. The activation of P38 have been considered to affect the activation of STAT3[15], being also shown to regulate NFATc1 during osteoclastogenesis[16]. Therefore, we focused on the effect Pexmetinib of activation of STAT3. By the western blot results, Pexmetinib indeed attenuated RANKL-stimulated activating phosphorylation of STAT3 activation (Fig. 3 **C-D**). Furthermore, we used a chromosome immunoprecipitation (ChIP) assay demonstrated that Pexmetinib reduced the bind capacity of STAT3 on the promoter region of NFATc1 (Fig. 3**E**). These results suggest that Pexmetinib suppressed osteoclast formation may partly via suppressing p38-STAT3-NFATc1 axis.

Next, we performed the rescue experiments to confirm our finding, we treated BMMs with Colivelin (an activator of STAT3) following

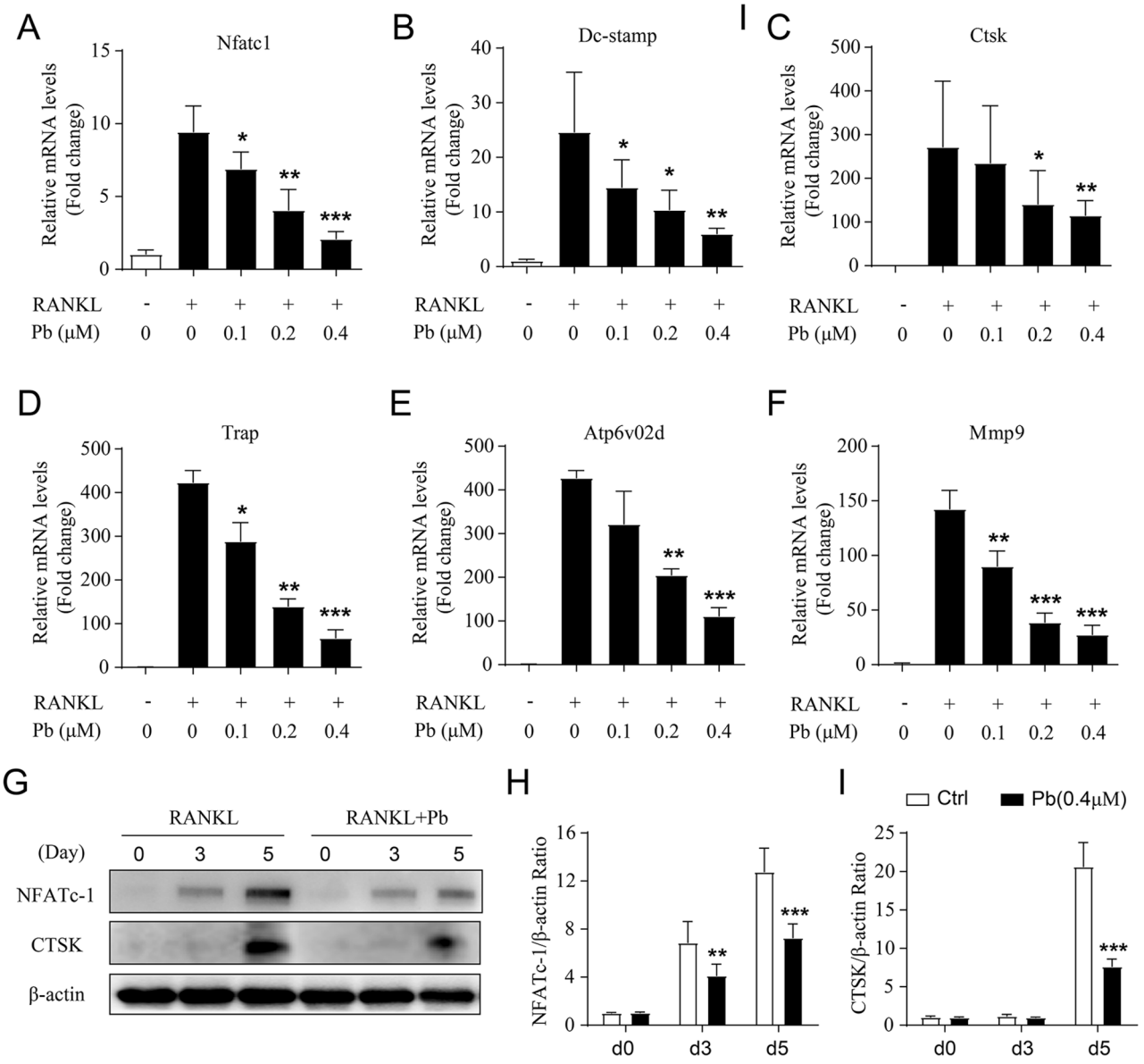

Fig. 2. Pexmetinib suppressed osteoclastic gene expression via down-regulating NFATc1. (A-F) *Nfatc1*, *Dc-stamp*, *Trap*, *Ctsk* and *Mmp-9* gene expression in BMMs treated with different doses of Pexmetinib (0, 0.1, 0.2, 0.4 μM) for 5 days under RANKL stimulation were analyzed by real-time PCR. RNA expression levels were normalized relative to the expression of *Gapdh*. **(G)** NFATc1 and CTSK protein levels in BMMSs treated with or without Pexmetinib for 0, 3 and 5 days were determined by Western blotting. **(H-I)** The grey levels of NFATc1 and CTSK was quantified and normalized to GAPDH using Image J. *P < 0.05; **P < 0.01. Data are expressed as means ± SEM, n = 5.

treatment with Pexmetinib. As shown in Fig. 4**F-G**, osteoclast formation was inhibited under Pexmetinib treatment, whereas the impaired osteoclastogenesis was partially rescued in the present with Colivelin treatment. Consistent with the previous results, the protein expressions of NFATc1 and TRAP were also partially rescuedby Colivelin (Fig. 3**H-I**). Collectively, these data suggested that Pexmetinib primarily modulated STAT3 activation, further affecting NFATc1 expression during osteoclast formation.

3.4. *Pexmetinib exerted anti-tumor effects in breast cancer cells in vitro*

After clarifying the role of Pexmetinib on osteoclast differentiation and function, the effects of Pexmetinib on the viability, migration, invasion of MDA-MB-231 cells were evaluated. MDA-MB-231 cells were treated with Pexmetinib (0–60 μM) for 48 and 96 h, and cell viability was determined by the CCK-8 assay (Fig. 4**A-B**). And the inhibitory concentration (IC)50 value of Pexmetinib at 96 h was shown to be 17.43 μM (Fig. 4**C**).

Next, we investigated the effects of Pexmetinib on cell migration and invasion by Transwell assay (Fig. 4**D**). Pexmetinib inhibited MDA-MB-231 cell migration and invasion in concentration-dependent manners (Fig. 4**E**). Moreover, Pexmetinib treatment markedly inhibited the mRNA expression (Fig. 4**F**) and protein levels (Fig. 4**G-H**) of MMP-2 and MMP-9, which are the key proteases involved in tumor invasion and metastasis[17]. These results suggested that Pexmetinib exerted anti-tumor effects in breast cancer cells *in vitro*.

3.5. *Pexmetinib suppressed breast cancer cells metastasis by impairing p38-STAT3-MMPs axis.*

As Pexmetinib suppressed osteoclastogenesis by impairing STAT3 activation, we further to investigate whether Pexmetinib affected breast cancer cells by the modulation of STAT3 activation. The phosphorylation of p38 and STAT3 were repressed by Pexmetinib treatment in MDA-

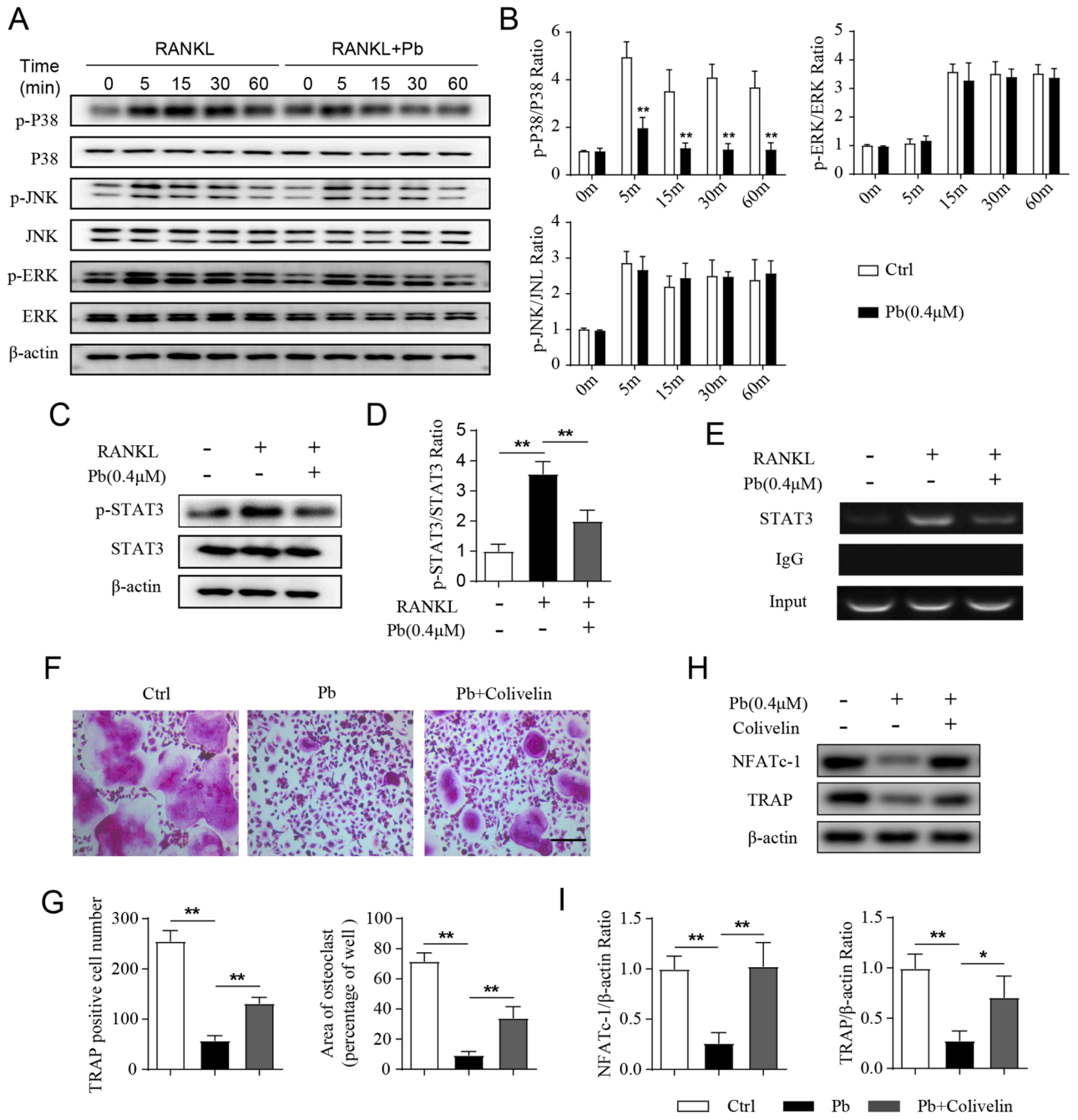

Fig. 3. Pexmetinib impaired p38-STAT3-NFATc1 axis during osteoclastogenesis. (A) (A) BMMs were pretreated with or without 0.4 μM Pexmetinib for 2 h before the addition of RANKL (50 ng/mL) for the indicated periods, the levels of indicated proteins were determined by Western blotting. **(B)** The grey levels of phosphorylated p38, JNK, ERK were quantified and normalized to total p38, JNK, ERK and β-actin using Image J. **(C)** BMMs were treated with or without 0.4 μM Pexmetinib under RANKL (50 ng/mL) stimulation. (D) The grey levels of phosphorylated STAT3 were quantified and normalized to total STAT3 and β-actin using Image J. **(E)** BMMs were treated with or without 0.4 μM Pexmetinib following stimulated with RANKL (50 ng/mL) for 48 h and then subjected to ChIP analysis. **(F-G)** BMMs were cultured by osteoclast differentiation medium for 5 days under Pexmetinib (0.4 μM) treatment or Pexmetinib (0.4 μM) + Colivelin (2 μM) treatment. Then cells were stained by TRAP and the number and areas of osteoclasts from were measured. **(H-I)** BMMs were treated as described in **F**, then the total proteins of cells were extracted. The levels of indicated proteins were determined by Western blotting. Scale bar = 100 μm, *P < 0.05; **P < 0.01. Data are expressed as means ± SEM, n = 5.

MB-231 cells (Fig. 5**A-B**). Interestingly, we also found that the inhibition of Pexmetinib on MDA-MB-231 cell migration and invasion were partly rescued by Colivelin treatment (Fig. 6**C-D**), accompanied with the rescue effect in MMP-2 and MMP-9 protein expression (Fig. 6**E-F**). There results suggest that Pexmetinib may suppressed breast cancer cells metastasis by impairing p38-STAT3-MMPs axis.Fig. 7..

3.6. Pexmetinib suppressed breast cancer cell-induced osteolytic lesions in vivo

Based on the inhibitory effects of Pexmetinib on osteoclastogenesis and breast cancer cells, we established an intra-tibial injection xeno-transplant model to test the effects of Pexmetinib on osteolytic bone damage caused by breast cancer cells (Fig. 6**A**). Tissue volume, tissue length, and tissue weight were reduced in the Pexmetinib group

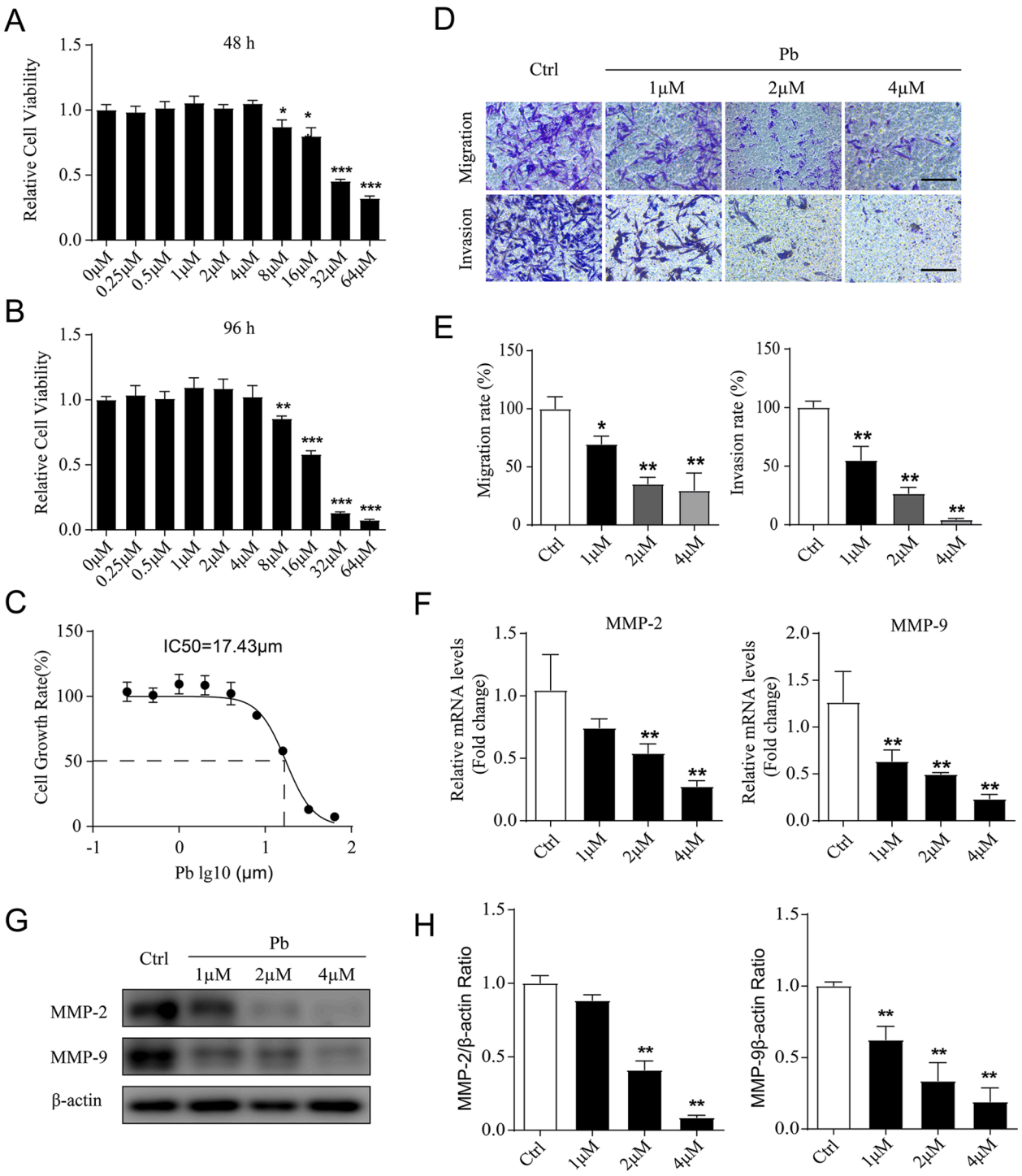

Fig. 4. Pexmetinib inhibited breast cancer cells migration and invasion *in vitro*. **(A, B)** Cell viability of Pexmetinib treated MDA-MB-231 cells were tested by CCK-8 assays at 48 and 96 h. **(C)** The IC50 value of Pexmetinib at 96 h on MDA-MB-231 cells. **(D)** The effects of Pexmetinib on MDA-MB-231 cells migration and invasion at a dose dependent manner were determined by transwell assay. **(E)** Migration and invasion rates were measured using Image J and normalized relative to the control group. **(F)** The MDA-MB-231 cells were treated with different doses of Pexmetinib (0, 1, 2, 4 μM) for 24 h. The gene expressions of *MMP-2* and *MMP-9* were tested by RT-PCR. **(G)** The MDA-MB-231 cells were treated with different doses of Pexmetinib (0, 1, 2, 4 μM) for 24 h. The western blot was performed to detected bond images of indicated proteins. **(H)** Quantitative analysis of protein gray levels related to β-actin by imageJ. Scale bar = 100 μm, *P < 0.05; **P < 0.01. Data are expressed as means ± SEM, n = 5.

compared with those in the vehicle group (Fig. 6**B**). This indicated that Pexmetinib effectively inhibited breast cancer bone metastasis and growth *in vivo*. The micro-CT analyses showed that osteolytic damage did not occur in the sham group, whereas breast cancer-induced osteolysis developed in the vehicle and Pexmetinib groups (Fig. 6**C**). However, Pexmetinib treatment decreased bone loss as evidenced by an increased trabecular BV/TV ratio and trabecular number, but reduced trabecular separation compared to controls (Fig. 6**D**). Similarly, H&E staining results suggest that more bone damage and tumor tissue appear in vehicle group than in the Pexmetinib treatment group (Fig. 6**E**). Moreover, the TRAP staining showed that TRAP-positive osteoclasts observed were quite less in the Pexmetinib treatment groups than in the

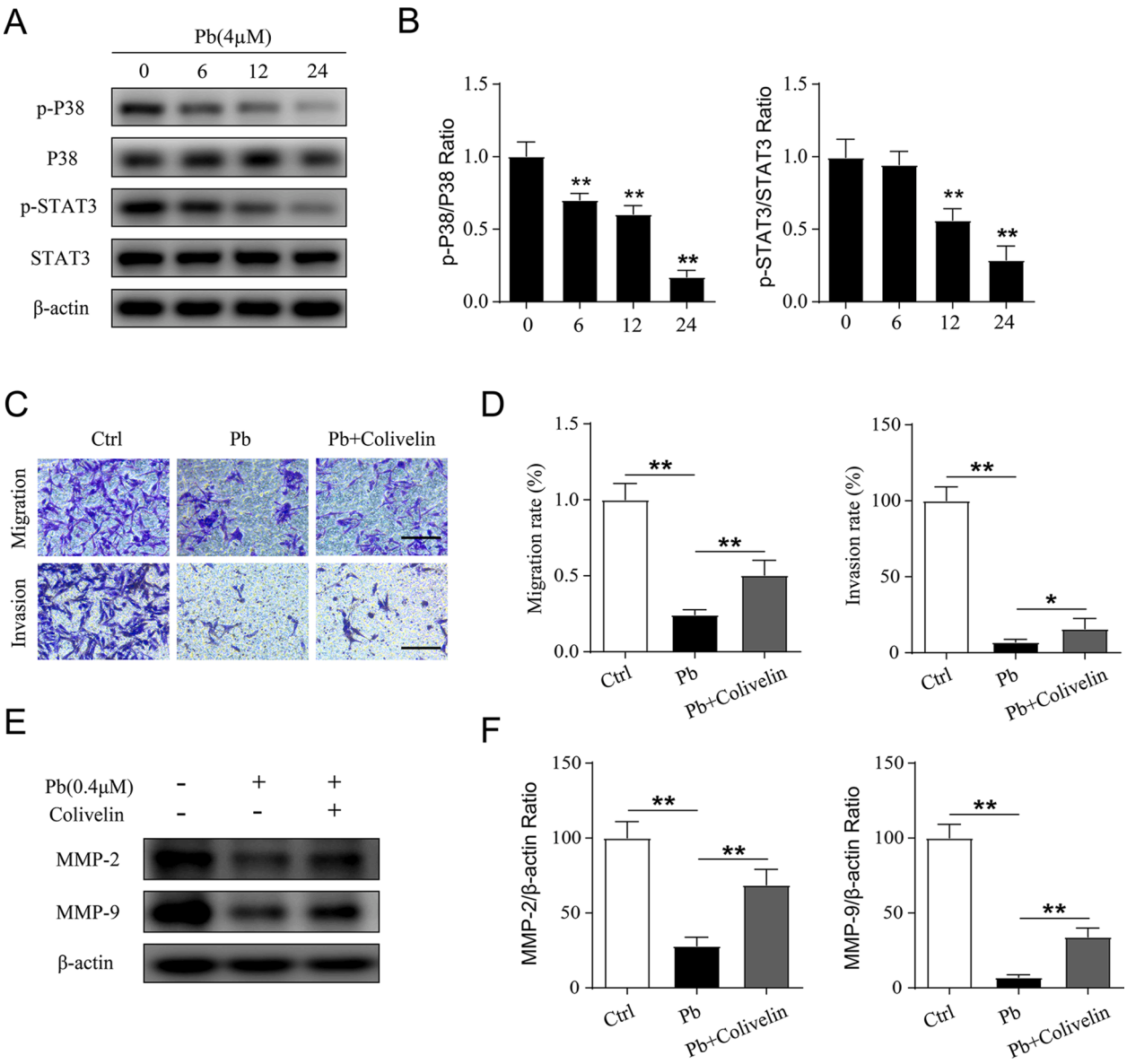

Fig. 5. Pexmetinib suppressed breast cancer cells metastasis by impairing p38-STAT3-MMPs axis. (A) MDA-MB-231 cells were treated with Pexmetinib (4 μM) for 0 h, 6 h, 12 h, 24 h, and the levels of the indicated proteins were determined by Western blotting. **(B)** The grey levels of p-p38, p-STAT3 were quantified and normalized to total p38, STAT3 and β-actin using Image J. **(C)** MDA-MB-231 cells were treated with Pexmetinib (4 μM) in the present with or without Colivelin, and cells migration and invasion were determined by transwell assay. **(D)** Migration and invasion rates were measured using Image J and normalized relative to the control group. **(E-F)** MDA-MB-231 cells were treatment with Pexmetinib (4 μM) in the present with or without Colivelin for 24 h, and the levels of MMP-2 and MMP-9 were determined by Western blotting. Scale bar = 100 μm, *P < 0.05; **P < 0.01. Data are expressed as means ± SEM, n = 5.

vehicle group (Fig. 6**F**). Meanwhile, Pexmetinib treatment was shown to inhibit osteoclastogenesis on non-tumor mice (Figure S1A-B). Furthermore, Immunohistochemical staining results demonstrated that the p-STAT3 were significantly reduced in the Pexmetinib treatment group compared with the vehicle group (Fig. 6**G**). In addition, we found Pexmetinib treatment has no biological toxicity on the liver and kidney of mice (Figure S2A). These results *in vivo* determined that Pexmetinib exhibited a potential therapeutic effect on breast cancer induced osteolysis.

4. Discussion

Breast cancer metastasizes to the bone with the development of osteolytic lesions can lead to a series of bone-related events that seriously affect the quality of life[1,2]. Although bisphosphonates and denosumab are effective in the treatment of breast cancer-induced osteolysis, alternative treatments should be considered due to the side effect of bisphosphonates and denosumab[9,18]. Previous data confirms that the p38 MAPK signaling pathway is involved in osteoclast formation and cancer-induced osteolysis[19,20]. Therefore, we found a novel p38 inhibitor Pexmetinib, which has been investigated in phase I clinical trials for treating myelodysplastic syndrome[13], may be an attractive compound for treating breast cancer-induced osteolysis.

P38 MAPK belong to a class of mitogen-activated protein kinases (MAPKs) that are responsive to RANKL stimulation during osteoclast differentiation[20]. Many transcription factors, including STAT3, are activated followed by P38 activation[15]. Moreover, some studies have demonstrated that STAT3 activation are involved in the early stages of osteoclast differentiation and regulated many osteoclatic gene expression, such as *NFATc1*[21]. Thus, RANKL stimulation contributes to the phosphorylation of P38 leading to the activation of STAT3, which may be an important step in the early process of osteoclast differentiation.

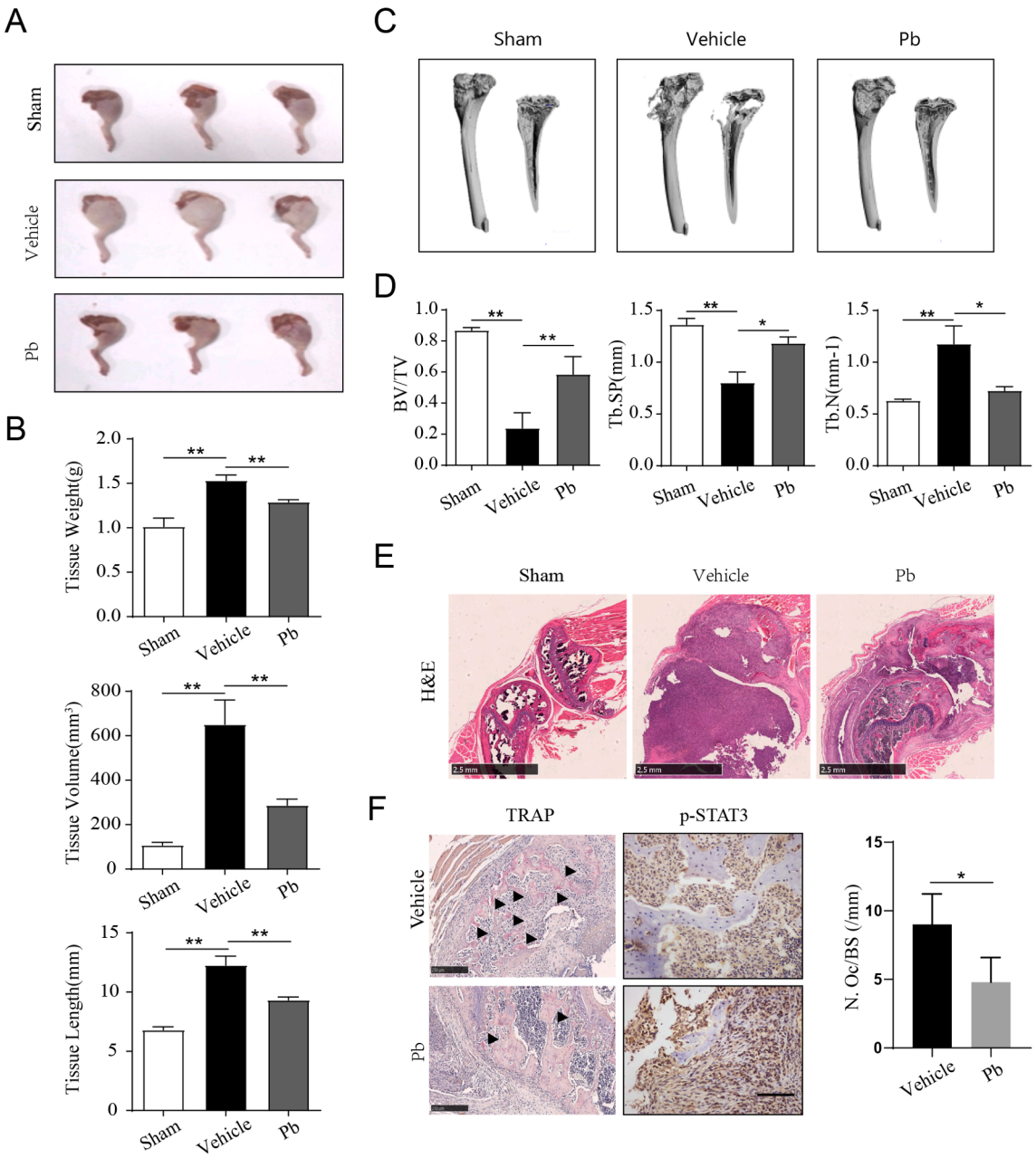

Fig. 6. Pexmetinib suppressed breast cancer cell-induced osteolytic lesions *in vivo*. **(A-B)** MDA-MB-231 cells were injected directly into the tibiae plateau. After 28 days of treatment, all mice were executed. The tissue volume, tissue width and tissue length were measured. **(C)** Three-dimensional reconstructed tibiae images are presented. **(D)** The BV/TV ratio, trabecular number (Tb.N), and trabecular separation (Tb.Sp) of each sample was measured. **(E-F)** The tibiae sections were stained with H&E, TRAP and p-STAT3 immunohistochemical staining. Scale bar = 200 μm, *P < 0.05; **P < 0.01. Data are expressed as means ± SEM, n = 5.

Consistent with this, we found that Pexmetinib inhibited RANKL-activated phosphorylation of p38, accompanied by impaired activation STAT3. These results suggested that Pexmetinib suppressed osteoclast differentiation may through inhibiting p38-STAT3-NFATc1 axis. Further ChIP assay and rescue assay confirmed it.

STAT3 is constitutively activated in numerous cancer types, including breast cancers[22,23]. Hyperactivated STAT3 contributes malignant progression through the regulation of key genes expression, including cell survival proteins such as Bcl-2[24,25], cell growth proteins such as cyclin D1/D2[26], inducers of angiogenesis such as vascular endothelial growth factor[27], and stimulators of invasion and metastasis such as MMP-2, MMP-9[28–30]. Therefore, we suspected that Pexmetinib exerted anti-tumor effects through inhibiting p38-STAT3 axis in breast cancer. We found that Pexmetinib inhibited cells proliferation, migration and invasion *in vitro*, and down-regulated the phosphorylation of P38 and STAT3 activation in breast cancer cells, following by the down-regulation of MMP-2 and MMP-9 expression.

Meanwhile, there are still some limitations to this study. The movement of cells from the primary tumor to the bone is a very complex process. However, our animal model simply reconstructed the destruction of bone in the local environment of breast cancer cells. In addition, Pexmetinib, though a p38 MAPK inhibitor, also inhibits the angiopoietin-1 receptor, TIE-2[31]. It's worthy of our further exploration that TIE-2 may be as a therapeutic target for controlling tumor angiogenesis and osteolytic bone metastasis in breast cancer[31,32].

In summary, we have demonstrated that a novel inhibitor, Pexmetinib suppresses osteoclastogenesis and tumorigenesis by suppressing the activity of STAT3, thereby contributing to the impairment of breast

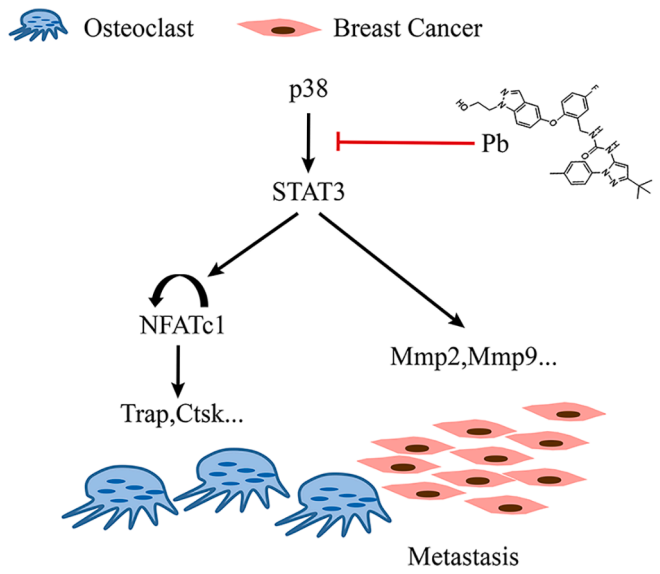

Fig. 7. Pexmetinib suppresses osteoclast formation and breast cancer metastasis via P38/STAT3 signal pathway. A graph abstract showing the working model of the role of Pexmetinib in inhibiting osteoclastogenesis and breast cancer metastasis.

cancer-induced osteolysis *in vivo*. Our findings provided a promising drug for repositioning toward the treatment of breast cancer-induced osteolysis.

Declaration of Competing Interest

The authors declare that they have no known competing financial interests or personal relationships that could have appeared to influence the work reported in this paper.

Acknowledgments

Thanks all support from department of Orthopaedics, Sir Run Run Shaw Hospital, School of Medicine, Zhejiang University. The authors are grateful to all staffs who contributed to this study.

Funding

This study was sponsored by the National Natural Science Fund of China (81772387; 81472064).

Author Contributions

JZW, WSY, XZA and JC conceived and designed the experiments. JZW, XZA, WSY, JC and ZXD performed the experiments. JZW, XZA, YHJ and WSY conducted the animal study. JZW, XZA, JC and YHJ analyzed the data. XZA and JC supervised the experiments. JZW and XZA drafted the manuscript. JC and YHJ revised the manuscript. All authors approved the final version of the manuscript.

Appendix A. Supplementary data

Supplementary data to this article can be found online at https://doi.org/10.1016/j.jbo.2022.100439.

References

[1] K.M. Bussard, C.V. Gay, A.M. Mastro, The bone microenvironment in metastasis; what is special about bone? Cancer Metastasis Rev. 27 (1) (2008) 41–55.
[2] G.R. Mundy, Metastasis to bone: causes, consequences and therapeutic opportunities, Nat. Rev. Cancer 2 (8) (2002) 584–593.
[3] N. Brook, E. Brook, A. Dharmarajan, C.R. Dass, A. Chan, Breast cancer bone metastases: pathogenesis and therapeutic targets, Int. J. Biochem. Cell Biol. 96 (2018) 63–78.
[4] P.S. Steeg, Tumor metastasis: mechanistic insights and clinical challenges, Nat. Med. 12 (8) (2006) 895–904.
[5] W.J. Boyle, W.S. Simonet, D.L. Lacey, Osteoclast differentiation and activation, Nature 423 (6937) (2003) 337–342.
[6] K. Ishiyama, T. Yashiro, N. Nakano, K. Kasakura, R. Miura, M. Hara, F. Kawai, K. Maeda, N. Tamura, K. Okumura, H. Ogawa, Y. Takasaki, C. Nishiyama, Involvement of PU.1 in NFATc1 promoter function in osteoclast development, Allergology international : official journal of the Japanese Society of Allergology 64 (3) (2015) 241–247.
[7] W. Kozlow, T.A. Guise, Breast cancer metastasis to bone: mechanisms of osteolysis and implications for therapy, J. Mammary Gland Biol. Neoplasia 10 (2) (2005) 169–180.
[8] Y. Liu, S. Zhao, W. Chen, F. Hu, L. Zhu, Q. Zhang, Y. Zhao, Bisphosphonate use and the risk of breast cancer: a meta-analysis of published literature, Clin. Breast Cancer 12 (4) (2012) 276–281.
[9] S.H. Tan, S. Saseendar, B.H. Tan, A. Pawaskar, V.P. Kumar, Ulnar fractures with bisphosphonate therapy: a systematic review of published case reports, Osteoporos. Int. 26 (2) (2015) 421–429.
[10] M. Cargnello, P.P. Roux, Activation and function of the MAPKs and their substrates, the MAPK-activated protein kinases, Microbiol. Mol. Biol. Rev. 75 (1) (2011) 50–83.
[11] D. Lu, J. Li, H. Liu, G.E. Foxa, K. Weaver, J. Li, B.O. Williams, T. Yang, LRP1 Suppresses Bone Resorption in Mice by Inhibiting the RANKL-Stimulated NF-κB and p38 Pathways During Osteoclastogenesis, J. Bone Miner. Res. 33 (10) (2018) 1773–1784.
[12] J. Yang, J. He, J. Wang, Y. Cao, J. Ling, J. Qian, Y. Lu, H. Li, Y. Zheng, Y. Lan, S. Hong, J. Matthews, M.W. Starbuck, N.M. Navone, R.Z. Orlowski, P. Lin, L. W. Kwak, Q. Yi, Constitutive activation of p38 MAPK in tumor cells contributes to osteolytic bone lesions in multiple myeloma, Leukemia 26 (9) (2012) 2114–2123.
[13] G. Garcia-Manero, H.J. Khoury, E. Jabbour, J. Lancet, S.L. Winski, L. Cable, S. Rush, L. Maloney, G. Hogeland, M. Ptaszynski, M.C. Calvo, Z. Bohannan, A. List, H. Kantarjian, R. Komrokji, A phase I study of oral ARRY-614, a p38 MAPK/Tie2 dual inhibitor, in patients with low or intermediate-1 risk myelodysplastic syndromes, Clin. Cancer. Res. 21 (5) (2015) 985–994.
[14] Z. Xie, H. Yu, X. Sun, P. Tang, Z. Jie, S. Chen, J. Wang, A. Qin, S. Fan, A Novel Diterpenoid Suppresses Osteoclastogenesis and Promotes Osteogenesis by Inhibiting Ifrd1-Mediated and IκBα-Mediated p65 Nuclear Translocation, J. Bone Miner. Res. 33 (4) (2018) 667–678.
[15] J.G. Bode, C. Ehlting, D. Häussinger, The macrophage response towards LPS and its control through the p38(MAPK)-STAT3 axis, Cell. Signal. 24 (6) (2012) 1185–1194.
[16] Y. Yang, M.R. Chung, S. Zhou, X. Gong, H. Xu, Y. Hong, A. Jin, X. Huang, W. Zou, Q. Dai, L. Jiang, STAT3 controls osteoclast differentiation and bone homeostasis by regulating NFATc1 transcription, J. Biol. Chem. 294 (42) (2019) 15395–15407.
[17] N.M. Hooper, Y. Itoh, H. Nagase, Matrix metalloproteinases in cancer, Essays Biochem. 38 (2002) 21–36.
[18] C. Reyes, M. Hitz, D. Prieto-Alhambra, B.o. Abrahamsen, Risks and Benefits of Bisphosphonate Therapies, J. Cell. Biochem. 117 (1) (2016) 20–28.
[19] H. Liu, J. He, J. Yang, Tumor cell p38 MAPK: A trigger of cancer bone osteolysis, Cancer cell & microenvironment 2 (1) (2015).
[20] K. Lee, I. Seo, M. Choi, D. Jeong, Roles of Mitogen-Activated Protein Kinases in Osteoclast Biology, Int. J. Mol. Sci. 19 (10) (2018) 3004.
[21] C.H. Li, L.L. Xu, L.L. Jian, R.H. Yu, J.X. Zhao, L. Sun, G.H. Du, X.Y. Liu, Stattic inhibits RANKL-mediated osteoclastogenesis by suppressing activation of STAT3 and NF-κB pathways, Int. Immunopharmacol. 58 (2018) 136–144.
[22] S.R. Walker, M. Xiang, D.A. Frank, Distinct roles of STAT3 and STAT5 in the pathogenesis and targeted therapy of breast cancer, Mol. Cell. Endocrinol. 382 (1) (2014) 616–621.
[23] K. Banerjee, H. Resat, Constitutive activation of STAT3 in breast cancer cells: A review, Int. J. Cancer 138 (11) (2016) 2570–2578.
[24] S. Alas, B. Bonavida, Rituximab inactivates signal transducer and activation of transcription 3 (STAT3) activity in B-non-Hodgkin's lymphoma through inhibition of the interleukin 10 autocrine/paracrine loop and results in down-regulation of Bcl-2 and sensitization to cytotoxic drugs, Cancer Res. 61 (13) (2001) 5137–5144.
[25] T. Gritsko, A. Williams, J. Turkson, S. Kaneko, T. Bowman, M. Huang, S. Nam, I. Eweis, N. Diaz, D. Sullivan, S. Yoder, S. Enkemann, S. Eschrich, J.H. Lee, C. A. Beam, J. Cheng, S. Minton, C.A. Muro-Cacho, R. Jove, Persistent activation of stat3 signaling induces survivin gene expression and confers resistance to apoptosis in human breast cancer cells, Clin. Cancer. Res. 12 (1) (2006) 11–19.
[26] J.E. Darnell Jr., Transcription factors as targets for cancer therapy, Nat. Rev. Cancer 2 (10) (2002) 740–749.
[27] G. Niu, K.L. Wright, M. Huang, L. Song, E. Haura, J. Turkson, S. Zhang, T. Wang, D. Sinibaldi, D. Coppola, R. Heller, L.M. Ellis, J. Karras, J. Bromberg, D. Pardoll, R. Jove, H. Yu, Constitutive Stat3 activity up-regulates VEGF expression and tumor angiogenesis, Oncogene 21 (13) (2002) 2000–2008.
[28] T.X. Xie, F.J. Huang, K.D. Aldape, S.H. Kang, M. Liu, J.E. Gershenwald, K. Xie, R. Sawaya, S. Huang, Activation of stat3 in human melanoma promotes brain metastasis, Cancer Res. 66 (6) (2006) 3188–3196.
[29] T.N. Dechow, L. Pedranzini, A. Leitch, K. Leslie, W.L. Gerald, I. Linkov, J. F. Bromberg, Requirement of matrix metalloproteinase-9 for the transformation of human mammary epithelial cells by Stat3-C, Proc. Natl. Acad. Sci. U. S. A. 101 (29) (2004) 10602–10607.

[30] T.X. Xie, D. Wei, M. Liu, A.C. Gao, F. Ali-Osman, R. Sawaya, S. Huang, Stat3 activation regulates the expression of matrix metalloproteinase-2 and tumor invasion and metastasis, Oncogene 23 (20) (2004) 3550–3560.
[31] L. Bachegowda, K. Morrone, S.L. Winski, I. Mantzaris, M. Bartenstein, N. Ramachandra, O. Giricz, V. Sukrithan, G. Nwankwo, S. Shahnaz, T. Bhagat, S. Bhattacharyya, A. Assal, A. Shastri, S. Gordon-Mitchell, A. Pellagatti, J. Boultwood, C. Schinke, Y. Yu, C. Guha, J. Rizzi, J. Garrus, S. Brown, L. Wollenberg, G. Hogeland, D. Wright, M. Munson, M. Rodriguez, S. Gross, D. Chantry, Y. Zou, L. Platanias, L.E. Burgess, K. Pradhan, U. Steidl, A. Verma, Pexmetinib: A Novel Dual Inhibitor of Tie2 and p38 MAPK with Efficacy in Preclinical Models of Myelodysplastic Syndromes and Acute Myeloid Leukemia, Cancer Res. 76 (16) (2016) 4841–4849.
[32] Y. Min, X. Ren, D.B. Vaught, J. Chen, E. Donnelly, C.C. Lynch, P.C. Lin, Tie2 signaling regulates osteoclastogenesis and osteolytic bone invasion of breast cancer, Cancer Res. 70 (7) (2010) 2819–2828.